Local and Global Ligand-Induced Changes in the Structure of the $GABA_A$ Receptor†

Yukiko Muroi, Cynthia Czajkowski, and Meyer B. Jackson*

Department of Physiology and Molecular and Cellular Pharmacology Program, University of Wisconsin School of Medicine, 1300 University Avenue, Madison, Wisconsin 53706

Received February 2, 2006; Revised Manuscript Received April 18, 2006

ABSTRACT: Ligand-gated channels mediate synaptic transmission through conformational transitions triggered by the binding of neurotransmitters. These transitions are well-defined in terms of ion conductance, but their structural basis is poorly understood. To probe these changes in structure, $GABA_A$ receptors were expressed in *Xenopus* oocytes and labeled at selected sites with environment-sensitive fluorophores. With labels at two different residues in the α_1 subunit in loop E of the GABA-binding pocket, GABA elicited fluorescence changes opposite in sign. This pattern of fluorescence changes is consistent with a closure of the GABA-binding cavity at the subunit interface. The competitive antagonist SR-95531 inverted this pattern of fluorescence change, but the noncompetitive antagonist picrotoxin failed to elicit optical signals. In response to GABA (but not SR-95531), labels at the homologous residues in the β_2 subunit showed the same pattern of fluorescence change as the α_1-subunit labels, indicating a global transition with comparable movements in homologous regions of different subunits. Incorporation of the γ_2 subunit altered the fluorescence changes of α_1-subunit labels and eliminated them in β_2-subunit labels. Thus, the ligand-induced structural changes in the $GABA_A$ receptor can extend over considerable distances or remain highly localized, depending upon subunit composition and ligand.

Ligand-gated ion channels (LGICs)[1] are allosteric proteins that allow neurotransmitters and drugs to control the ion permeability of cell membranes. When ligands bind to these proteins, their channels open and close as the LGIC interconverts between distinct functional states. Most studies of these interconversions employ electrophysiological techniques, which provide relatively little insight into the structural basis of these transitions. Techniques that provide more detailed structural insight into ion-channel gating include the substituted-cysteine accessibility method (SCAM) and a variety of photometric methods. Experiments with SCAM identified patterns of solvent accessibility of residues that line the pore (*1*−*4*), as well as residues in ligand-binding regions (*5*−*8*). Site-specific fluorescent labeling has enabled photometry to be used to probe the conformational changes in LGICs as they occur in real time. In the $GABA_C$ receptor, this approach revealed agonist-mediated molecular rearrangements at three different locations (*9*). The muscle nicotinic acetylcholine receptor (nAChR) has been studied by similar techniques, revealing fluorescence changes during receptor activation and desensitization. A fluorophore attached near the extracellular end of the M2 segment of the nAChR channel provided insight into the gating pathways taken by the receptor when it was activated by different ligands (*10*).

The $GABA_A$ receptors, along with their relatives, the nAChRs, the glycine receptor, and the 5-HT_3 receptor, are pentamers composed of homologous subunits in a circular arrangement around a central axis (*11*). All of the subunits that form these receptors contain a large extracellular N terminus of about 200 amino acids, four transmembrane domains (M1−M4), and a small extracellular C terminus. The N terminus forms a sandwich of β sheets, which harbors the binding sites for neurotransmitters and many drugs (*12*−*14*). Residues in and flanking the M2 segments reside on a water-accessible surface that forms the transmembrane channel (*2*, *3*, *15*−*17*).

Recent crystallographic analysis of a molluscan acetylcholine-binding protein (AChBP) provided a three-dimensional structure with atomic resolution (*18*). AChBP shows a strong homology with the large N-terminal extracellular domain of the nAChR, and thanks to the homology among related LGICs, this structure has served as a valuable guide for structure−function studies of $GABA_A$ receptors. In addition, fluorescent labeling, intrinsic tryptophan fluorescence, and molecular dynamics studies of AChBP have provided considerable insight into the molecular rearrangements induced by ligands (*19*, *20*). The $GABA_A$ receptor and the AChBP employ homologous regions in the binding of ligands (*13*, *18*), and site-directed mutagenesis and affinity-labeling data have been incorporated into the AChBP structure to map out ligand-binding cavities of the $GABA_A$ receptor at the subunit interfaces (*12*−*14*, *21*).

† This work was supported by the UW/HHMI Research Resources Program and by NIH Grant NS34727.

* To whom correspondence should be addressed. Telephone: (608) 262-9111. Fax: (608) 262-9072. E-mail: mjackson@physiology.wisc.edu.

[1] Abbreviations: LGIC, ligand-gated ion channel; SCAM, substituted-cysteine accessibility method; nAChR, nicotinic acetylcholine receptor; AChBP, acetylcholine-binding protein; TMRM, tetramethylrhodamine maleimide; AF, Alexa Fluor 546 maleimide; MTSR, sulforhodamine methanethiosulfonate.

10.1021/bi060222v CCC: $33.50
Published on Web 05/19/2006

LGICs are symmetric or pseudosymmetric allosteric proteins, for which the Monod−Wyman−Changeux model postulates cooperative transitions during which subunits preserve their symmetry (*22*). The Koshland−Nemethy−Filmer model is often taken as a contrasting theory, where individual subunits are postulated to move independently, so that symmetry can be broken (*23*). Recent molecular dynamics simulations of the ligand-binding domain of the α7 nicotinic receptor suggested that without acetylcholine the five subunits adopt an asymmetric arrangement, which becomes more symmetric when acetylcholine binds (*24*). To gain insight into the structural basis of functional transitions in LGICs and to test some of the basic assumptions about subunit symmetry, we used site-specific fluorescent labels to study conformational changes at selected locations of the $GABA_A$ receptor. This allowed us to probe the conformational changes localized to these parts of the protein. Applying GABA along with competitive and noncompetitive $GABA_A$ receptor antagonists indicated that different drugs can induce conformational changes that are either restricted to the ligand-binding pocket or are distributed over a large portion of the extracellular domain of the receptor.

EXPERIMENTAL PROCEDURES

Molecular Biology. Cysteines were introduced by site-directed mutagenesis into the rat α_1 (E122, L127), β_2 (P120, L125), and γ_2 (N135, L140) subunits in the pGH19 vector (*25*). DNA sequencing confirmed the mutations. mRNA was prepared with the mMessage T_7 RNA polymerase transcription kit (Ambion, Austin, TX).

Oocyte Expression. Oocytes were removed from anesthetized *Xenopus laevis* and prepared as described previously (*26*). We generally injected smaller amounts of mRNA for studies of the concentration dependence of current (EC_{50} determination) and larger amounts for fluorescence. For expression of wild-type $\alpha\beta$ receptors, mRNA was injected in a ratio of 1:1 α/β (0.7 ng/subunit for EC_{50} determination from the current and 6.75 ng/subunit for fluorescence). mRNA was injected in a ratio of 2.5:1 α/β for α_1-subunit mutants (0.7−1.7 ng/subunit for EC_{50} determination from the current and 6.7−18 ng/subunit for fluorescence) and a ratio of 1:6 α/β for β_2-subunit mutants (0.7−4.2 ng/subunit for EC_{50} determination from the current and 4.5−27 ng/subunit for fluorescence). When the wild-type γ_2 subunit was included, the ratio was 1:1:8 ($\alpha/\beta/\gamma$; 0.7−5.4 ng/subunit for EC_{50} and 2.2−18 ng/subunit for fluorescence). The $\alpha/\beta/\gamma$ mRNA ratio was 8:1:8 for α_1-subunit mutations, 1:8:8 for β_2-subunit mutations, and 1:1:10 for γ_2-subunit mutations (0.68−6.8 ng/subunit mRNA for EC_{50} and 1.5−13.5 ng/subunit for fluorescence). Oocytes were incubated in ND96 solution (96 mM NaCl, 2 mM KCl, 1.8 mM $CaCl_2$, 1 mM $MgCl_2$, 5 mM HEPES at pH 7.4) at 18 °C for 3−6 days prior to experiments.

Fluorophore Labeling. Oocytes were incubated in 10 μM Alexa Fluor 546 maleimide (AF; Molecular Probes, Eugene, OR) in ND96 for 1 h at room temperature (*9*). Sulforhodamine methanethiosulfonate (MTSR; Toronto Research Chemical, Inc.) and tetramethylrhodamine maleimide (TMRM; Molecular Probes) labeling was carried out on ice for 30 min with 10 μM for each fluorescent reagents (*10*, *27*). Oocytes were washed with ND96 after labeling and used immediately for recording.

Two-Electrode Voltage Clamp. Recordings were performed at room temperature on oocytes voltage-clamped at −80 mV with an OC-725C Oocyte Clamp (Warner, Hamden, CT). An oocyte was placed in a chamber that allows constant flow of solution (∼4 mL/min), and this flow rate was maintained as solutions were changed with electronically controlled flow valves. We perfused with the control solution for at least 5 min between drug applications, and this time was extended to as long as 20 min after applying higher concentrations. The oocyte was perfused with ND96 and solutions of GABA, SR-95531, picrotoxin (Sigma, St. Louis, MO), and flurazepam (RBI, Natick, MA) in ND96. Stock solutions of picrotoxin were prepared in DMSO.

Glass electrodes filled with 3 M KCl had resistances of 0.2−2.0 MΩ. Incorporation of the γ_2 subunit was tested by co-application of a low concentration of GABA (EC_{10-20}) and flurazepam (*26*). Concentration−response curves were fitted to the following equation: $y = V_{max}(x^n/(EC_{50}{}^n + x^n))$ using Origin (Microcal Software, Inc., Northampton, MA), with V_{max} = maximum current, x = concentration, EC_{50} = the concentration of drug giving a half-maximal response, and n = Hill coefficient. Antagonist concentrations were selected to block GABA responses by at least 90%.

Simultaneous Current and Fluorescence Recording. Fluorescence was measured with a photomultiplier tube (Hamamatsu) coupled to a Nikon optiphot microscope. We used a 10× 0.50NA objective (Zeiss) and illuminated with a 100 W halogen lamp powered by a JQE power supply (Kepco, Flushing, NY). The same fluorescence filter set (535/50 excitation, dichroic mirror 565 LP, and 610/75 emission; Chroma Technology, Brattleboro, VT) was used for all three fluorophores. The voltage clamp and shutter were controlled by a Digidata interface and Clampex 8 (Axon Instruments/Molecular Devices, Sunnyvale, CA). The current signal was low-pass-filtered at 10−1000 Hz. Data were analyzed and graphed with Clampfit 8 and Origin. Fluorescence traces were corrected for bleaching, which made the baseline decay by an average of 0.15%/s. The pre- and postdrug fluorescence signals were fitted to an exponential function, which was then subtracted from the entire record. The gain was set at 10^7 V/A, giving a time constant of 150 ms with our current preamplifier (Oriel Instruments, Stratford, CT).

Structural Modeling. The structural model in Figure 1 was developed with Swiss Protein Bank Viewer (ca.expasy.ord/spdbv) starting with the AChBP structure (*18*) (RCSB Protein Data Base code 1I9B). The rat $GABA_A$ receptor sequences were aligned and threaded onto the AChBP tertiary structure, and the structure was energy-minimized as described previously (*8*). A $GABA_A$ receptor pentamer of extracellular domains ($\beta/\alpha/\beta/\alpha/\gamma$ viewed counterclockwise from the synaptic cleft) was assembled by overlaying the monomeric subunits on the AChBP scaffold. The resulting structure was imported into SYBYL (Tripos, Inc., St. Louis, MO) and energy-minimized with neither water nor entropy factors included. After the global energy minimization, Ramachandran plots, χ plots, side-chain positions, and cis and trans bonds were all examined. PROCHECK (*28*) was run to examine structural features against the established database of protein parameters, most importantly the ϕ/ψ torsions and side-chain conformations. Problems in the structure that were revealed by these evaluations were fixed manually, and energy minimizations were run again as needed. Regions

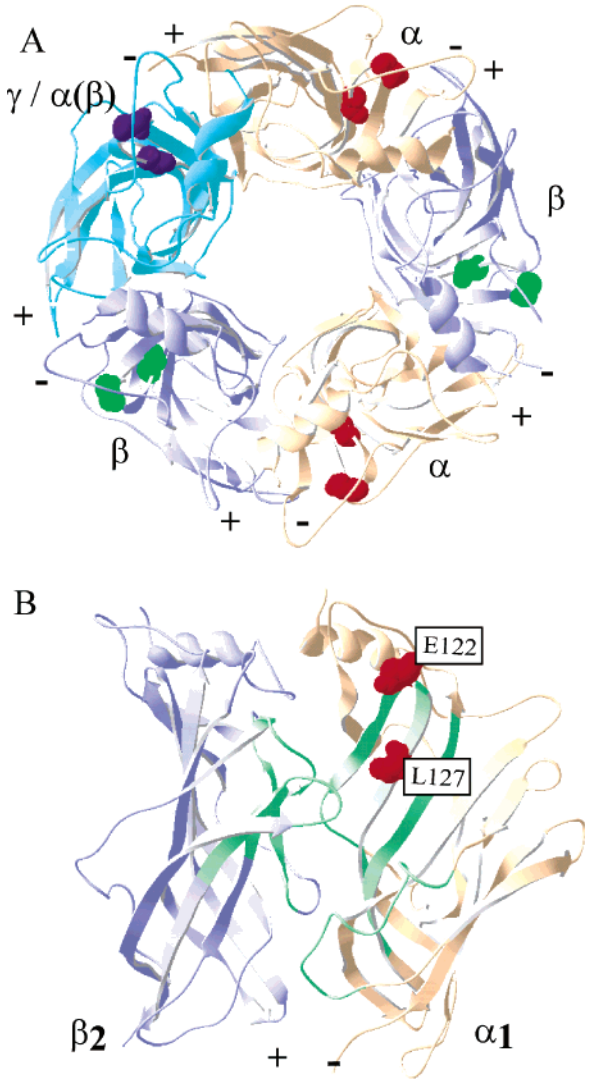

FIGURE 1: Structural models of the $GABA_A$ receptor. Models were based on the AChBP crystal structure (*18*), as adapted to the homologous extracellular domain of the $GABA_A$ receptor (see the Experimental Procedures). The ribbon representation of the backbone structure is used throughout, except that the mutated and labeled residues studied here (E122 and L127 in the α_1 subunit, red; P120 and L125 in the β_2 subunit, green; and N135 and L140 in the γ_2 subunit, dark blue) are represented as space filling. (A) Top view of the entire pentameric structure. A positive sign indicates the "principal" component of the binding pocket, and a negative sign indicates the "complementary" component (*29*). (B) Side view of the α subunit/β subunit interface containing the ligand-binding pocket, with the labeled residues on the α_1 subunit as space filling. The putative GABA-binding region is colored green (*8*). Note that the subunit labeled γ/α(β) would be a γ subunit when this subunit is included in the expression or either an α or β subunit when the γ subunit is omitted.

with insertions were modeled by fitting structures from a loop database. Because the sequence identity between the AChBP and the $GABA_A$ receptor ligand-binding domains is only about 18%, caution must be used in interpreting the absolute positions of individual side-chain residues in the model.

Statistical Analysis. Statistical analysis was performed using the *t* test and one-way analysis of variance (ANOVA) followed by the post-hoc Dunnett's test using GraphPad Prism (San Diego, CA). Analysis of EC_{50} values was performed following log transformation.

RESULTS

Label Sites. We selected two residues in the α_1 subunit for mutation to cysteine and labeling, E122 in β-strand 5′ and L127 in β-strand 6 (*18*), with both residues residing in loop E according to the terminology of Corringer et al. (*29*). Both of these residues are in the vicinity of the GABA-binding pocket (Figure 1B) and reside at the β_2/α_1-subunit interfaces in the extracellular domain (Figure 1A). The homologous residues in the β_2 subunit (P120, L125) and in the γ_2 subunit (N135, L140) were also labeled. SCAM studies have shown that GABA and the allosteric modulator, pentobarbital, changed the accessibility of the α_1-subunit residues selected for the present study, suggesting that this region undergoes a conformational change during activation (*30*, *31*). The residue homologous to L127 in the ρ_1 subunit of the $GABA_C$ receptor (L166) has also been labeled and shown to change its environment in response to GABA (*9*).

GABA-Induced Fluorescence Changes. Wild-type and mutant $\alpha_1\beta_2$ receptors (α_1E122C, α_1L127C, β_2P120C, and β_2L125C) were expressed in oocytes and labeled with the fluorescent sulfhydryl reagents AF, MTSR, or TMRM (see the Experimental Procedures). Examination of dose−response curves revealed that these mutations caused relatively modest changes in basic receptor function, except for α_1L127Cβ_2 (Table 1A), where the EC_{50} was much larger. Because this residue is closer to the GABA-binding site (Figure 1), its modification is more likely to interfere with GABA binding. Subsequent labeling produced shifts in the EC_{50} values, which were generally less than a factor of 2.

For each of these four mutants, the application of GABA elicited a change in the fluorescence of labels. These changes in fluorescence occurred simultaneously with the opening of channels (Figure 2). In control experiments with oocytes expressing wild-type receptors that had been treated with a label, no fluorescence changes were observed (see the top of Figure 5). Labels at α_1L127Cβ_2 (parts A and B of Figure 2) and the homologous residue $\alpha_1\beta_2$L125C (Figure 2E) reported increases in fluorescence in response to GABA, regardless of whether they were labeled with AF, MTSR, or TMRM. In contrast, labels at α_1E122Cβ_2 (parts C and D of Figure 2) and the homologous position $\alpha_1\beta_2$P120C (Figure 2F) showed a decrease in fluorescence. The simplest interpretation of these results is that the environments of these residues change polarity when the receptor is activated by GABA. According to this interpretation, α_1L127β_2 and $\alpha_1\beta_2$-L125 see a decrease in polarity and α_1E122β_2 and $\alpha_1\beta_2$P120 see an increase in polarity. The fluorescence traces in Figure 2 do not always return to baseline with the same time course as the current traces, but upon examining all of our records, we could not discern any clear trends. Although there may be valuable information about receptor kinetics from these features of the fluorescence changes, analyzing these processes will require a more careful study under conditions where drugs can be added and removed more rapidly.

The three different labels used here showed qualitatively similar behavior in reporting fluorescence changes at all four positions. Figure 3 shows the results for α-subunit labels. The linkages between the fluorophores and the cysteine side chain differed in length for these labels, with values of 15.1, 7.8, and 5.0 Å for AF, MTSR, and TMRM, respectively (determined with ACD/ChemSketch). Because MTSR and

Table 1: Concentration−Response Data for GABA Activation, before and after Fluorescent Labeling of $\alpha\beta$ (A) or $\alpha\beta\gamma$ (B) Receptors[a]

(A) $\alpha_1\beta_2$	unlabeled			AF labeled		
receptor	EC_{50} (μM)	Hill coefficient	*n*	EC_{50} (μM)	Hill coefficient	*n*
$\alpha_1\beta_2$	1.5 ± 0.4	1.18 ± 0.1	4	1.6 ± 0.4	1.21 ± 0.03	5
α_1(L127C)β_2	56.8 ± 9.5[b]	1.51 ± 0.3	6	94.6 ± 22.1[b]	0.91 ± 0.1	5
α_1(E122C)β_2	4.4 ± 1.4	0.96 ± 0.2	3	2.1 ± 0.3	1.35 ± 0.1	4
$\alpha_1\beta_2$(L125C)	0.9 ± 0.2	1.18 ± 0.1	4	1.6 ± 0.3	0.97 ± 0.2	3
$\alpha_1\beta_2$(P120C)	1.1 ± 0.3	1.10 ± 0.3	4	2.0 ± 0.4	0.75 ± 0.1	4
(B) $\alpha_1\beta_2\gamma_2$	unlabeled			TMRM labeled		
receptor	EC_{50} (μM)	Hill coefficient	*n*	EC_{50} (μM)	Hill coefficient	*n*
$\alpha_1\beta_2\gamma_2$	11.2 ± 1.1	1.01 ± 0.1	9	8.6 ± 1.2	1.02 ± 0.1	4
α_1(L127C)$\beta_2\gamma_2$	287 ± 19[b]	1.09 ± 0.1	6	354 ± 66[b]	1.26 ± 0.1	5
α_1(E122C)$\beta_2\gamma_2$	15.6 ± 2.7	1.15 ± 0.2	4	12.7 ± 0.6	1.11 ± 0.01	4
$\alpha_1\beta_2$(L125C)γ_2	24.7 ± 2.0[b]	1.19 ± 0.1	4	22.0 ± 4.1[b]	1.24 ± 0.1	5
$\alpha_1\beta_2$(P120C)γ_2	21.1 ± 3.5[b]	1.15 ± 0.04	6	32.4 ± 4.7[b]	1.38 ± 0.1	4
$\alpha_1\beta_2\gamma_2$(N135C)	40.3 ± 4.6[b]	1.04 ± 0.1	6	49.4 ± 6.4[b]	1.10 ± 0.1	4

[a] Mutant and wild-type receptors were expressed in oocytes. EC_{50} and Hill coefficient values were obtained from fits to the Hill equation (see the Experimental Procedures) of the indicated number of concentration−response plots. EC_{50} values were log-transformed, averaged, and anti-log-transformed to give final EC_{50} values. $\alpha\beta$ receptors were studied by expressing α_1- and β_2-subunit mRNA and labeling with AF. $\alpha\beta\gamma$ receptors were studied by expressing α_1-, β_2-, and γ_2-subunit mRNA and labeling with TMRM. [b] A statistically significant difference from the wild type by ANOVA ($p < 0.05$).

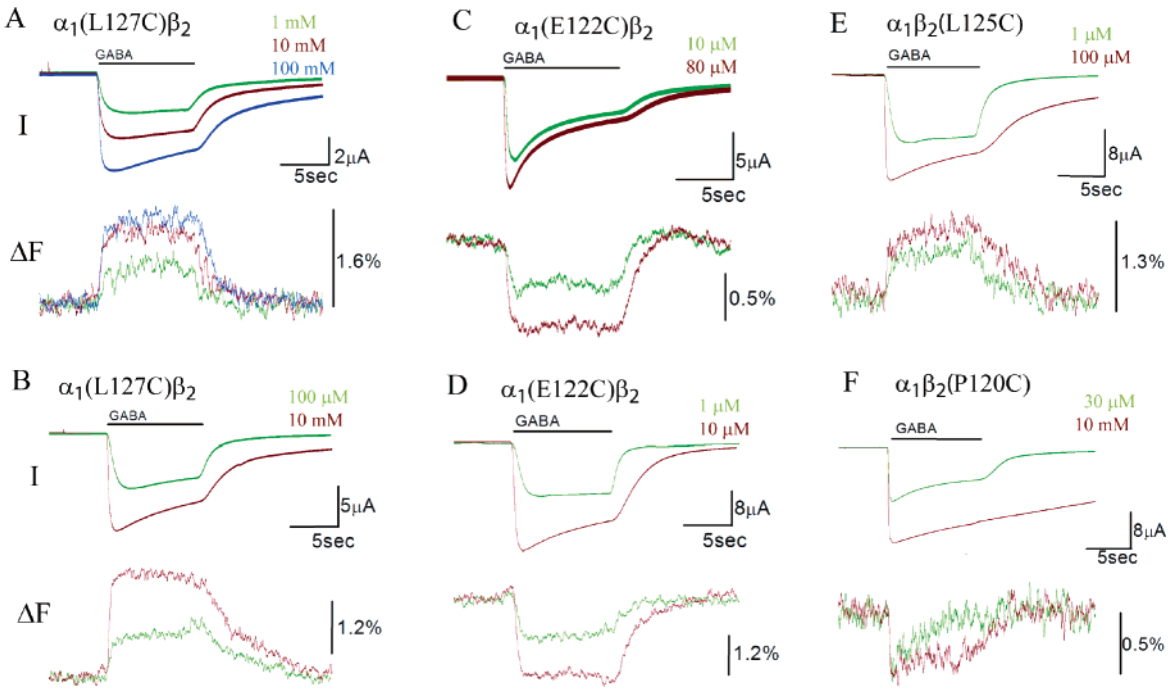

FIGURE 2: Simultaneous measurement of current and fluorescence changes in response to GABA. Current and fluorescence change in parallel when GABA was applied at the indicated concentrations. (A) α_1L127Cβ_2 receptors labeled with AF. (B) α_1L127Cβ_2 receptors labeled with MTSR. (C) α_1E122Cβ_2 receptors labeled with MTSR. (D) α_1E122Cβ_2 receptors labeled with TMRM. (E) $\alpha_1\beta_2$L125C receptors labeled with TMRM. (F) $\alpha_1\beta_2$P120C receptors labeled with AF. Because this label site tends to give small fluorescence changes, the magnitude of the change in this trace is greater than the average value indicated in Figure 5.

TMRM are both rhodamine labels, it may be significant that the greater fluorescence changes were seen with TMRM, which has the shorter linker. A shorter linker should allow structural changes on the receptor to impose greater changes on the environment of the fluorophore. Because the response was clearly larger with TMRM at α_1E122Cβ_2, this label was employed in the majority of our experiments. A less extensive comparison between labels at other sites also showed that TMRM gave the largest signals (data not shown).

Concentration−response curves of the current and fluorescence change were obtained from TMRM-labeled α_1E122Cβ_2 receptors (Figure 4). The two curves were superimposable after normalization, and the fits yielded indistinguishable parameter values (current: $EC_{50} = 1.5 \pm 0.3$ μM, Hill coefficient $= 1.3 \pm 0.03$ and ΔF: $EC_{50} = 1.4 \pm 0.5$ μM, Hill coefficient $= 1.2 \pm 0.1$). Other labels and sites showed the same trend, but quantitative comparisons were usually more difficult because of the smaller fluorescence changes.

Movements in Homologous Regions of the Extracellular Domain. A saturating concentration of GABA applied to $\alpha_1\beta_2$ receptors produced the same pattern of fluorescence change in labels on the homologous residues of the α_1 and β_2 subunits (Figures 2 and 5). This indicates that these homologous locations in very different parts of the protein undergo structural changes during receptor activation. The labeled sites on the β_2 subunit are quite remote from the

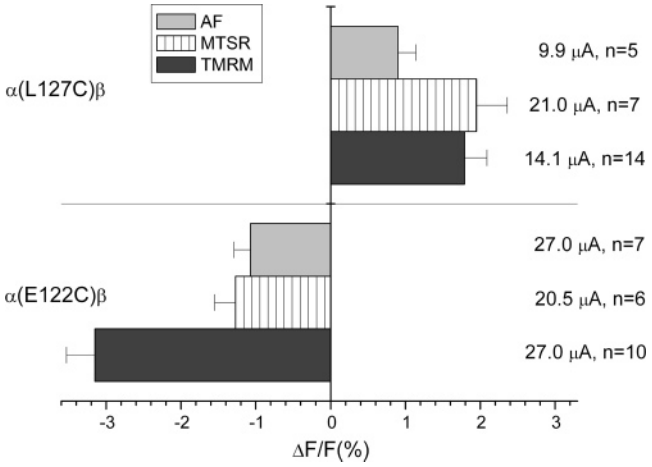

FIGURE 3: Average fluorescence changes observed with three different fluorescent labels. Mean ± standard error (SE) of fluorescence changes observed in response to GABA [EC_{90-99}] for AF-, MTSR-, and TMRM-labeled mutants (α_1L127Cβ_2 and α_1E122Cβ_2). Average peak GABA-activated current and number of oocytes are indicated on the right.

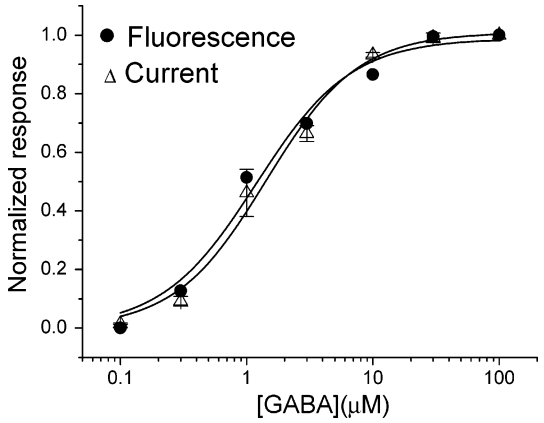

FIGURE 4: Concentration−response relationship of current and fluorescence in α_1E122Cβ_2 receptors. Concentration−response curves of GABA-activated current (△) and fluorescence (●) for TMRM-labeled α_1E122Cβ_2 receptors. Data were normalized to maximal responses and averaged for four experiments. The plot shows mean ± SE.

GABA-binding pocket lying at a subunit interface that is not involved in GABA binding (Figure 1A); therefore, this result indicates that the conformational transition induced by GABA binding extends over a considerable distance from the actual binding site. The similar pattern of fluorescence changes in the two pairs of labels raises the possibility of a transition with at least some degree of symmetry. However, both of the β_2-subunit labels showed smaller fluorescence changes than the corresponding α_1-subunit labels. This might in part reflect more labels on α_1 subunits, if the stoichiometry is $3\alpha_1 2\beta_2$. However, the differences probably also reflect the environments of the labels and the nature of the structural transition in the two subunits.

We examined $\alpha_1\beta_2\gamma_2$ receptors using wild-type and mutant γ_2 subunits. The concentration dependence of GABA-activated current was investigated before and after TMRM labeling (Table 1B). As in $\alpha\beta$ receptors, in $\alpha\beta\gamma$ receptors, the mutation α_1L127C$\beta_2\gamma_2$ produced a large increase in the EC_{50} value but the other mutations were closer to the wild type. Labeling these cysteine mutants with fluorophore did not alter the sensitivity of the receptor to GABA. With the

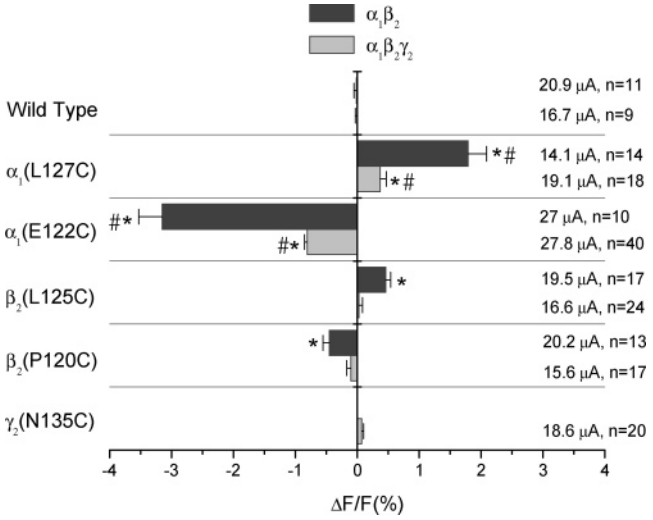

FIGURE 5: GABA-induced fluorescence changes in labeled receptors. GABA was applied at concentrations > EC_{90} to obtain near maximal fluorescence changes. The current was measured in parallel in each experiment. When the current was below 7 μA, fluorescence was not included in the average. Mean ± SE is shown for fluorescence with the mean current and number of oocytes to the right. $\alpha_1\beta_2\gamma_2$L140C receptors were not included because currents were too low (~300 nA). The maximal GABA-activated current and number of oocytes are indicated to the right. The asterisk and pound sign indicate a significant difference from the wild type by the *t* test and one-way ANOVA, respectively.

$\alpha_1\beta_2\gamma_2$L140C mutant, very small currents were seen (~300 nA); therefore, labeling and fluorescence measurements were not attempted.

Coexpression of the γ_2 subunit reduced the amplitude of the fluorescence changes in receptors with labels on the α_1 or β_2 subunits (Figure 5). We did not observe a fluorescence change in the label at position β_2L125C or β_2P120C when a γ_2 subunit was present. The current in oocytes expressing this receptor was quite high (average = 18.6 μA, Figure 5), indicating that expression levels were comparable to those seen in the absence of the γ_2 subunit. A label at $\alpha_1\beta_2\gamma_2$-N135C also showed no fluorescence change despite the large current (Figure 5). In these experiments, labeling was attempted for shorter time periods (1 min with MTSR) to reduce the background and detect smaller changes. However, in six experiments, no significant GABA-induced fluorescence change could be seen. We also tried labeling in the presence of GABA and still were unable to see a signal. Thus, this homologous residue in the γ_2 subunit may not undergo movements of the magnitude similar to that implied by the signals arising from labels on the α_1 and β_2 subunits. However, without a detectable fluorescence change, we cannot rule out the possibility that this site on the γ_2 subunit remains unlabeled. Indeed, we were unable to observe changes in flurazepam potentiation following TMRM treatment; therefore, failure to label this residue remains a distinct possibility.

A Comparison of the Open and Desensitized States. $GABA_A$ receptors, in common with the vast majority of LGICs, undergo desensitization in the continued presence of an agonist. The traces in Figure 2 suggest that the fluorescence does not change much as the receptor desensitizes, but in these experiments, the brief drug application times (10 s) limited the extent of desensitization. We therefore applied GABA for a longer time (20 s) to induce

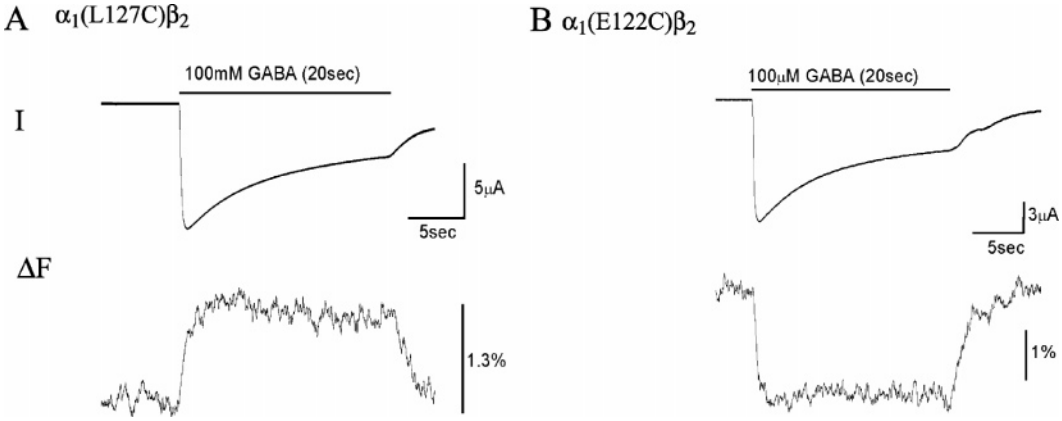

FIGURE 6: Desensitization in response to GABA. Parallel measurements of current and fluorescence during prolonged application of GABA (20 s) at the indicated concentrations. (A) α_1L127Cβ_2 receptors labeled with AF. (B) α_1E122Cβ_2 receptors labeled with TMRM. The fluorescence traces remain flat as the current declined because of desensitization. Note the longer application times compared to Figure 2.

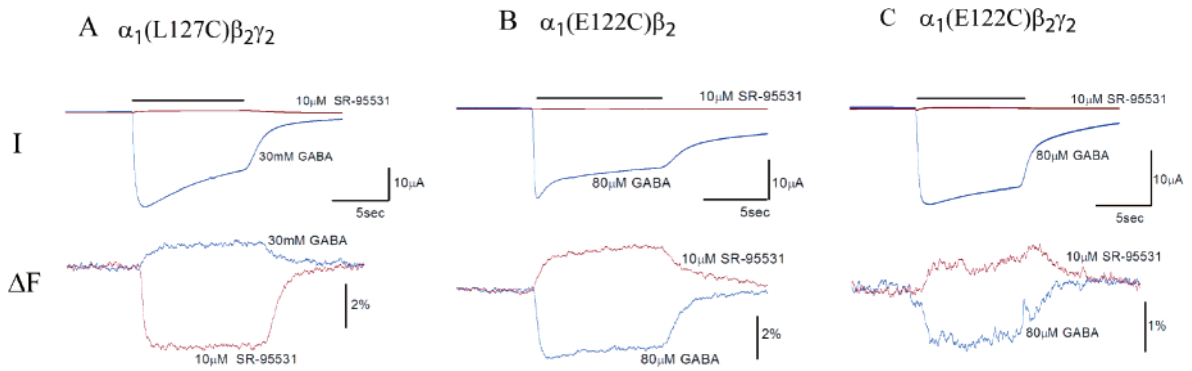

FIGURE 7: Current and fluorescence responses to GABA and SR-95531. Responses to GABA and the competitive antagonist, SR-95531, are shown in the same oocyte. The two drugs induced fluorescence changes in the opposite direction. (A) α_1L127C$\beta_2\gamma_2$ receptors labeled with TMRM. (B) α_1E122Cβ_2 receptors labeled with TMRM. (C) α_1E122C$\beta_2\gamma_2$ receptors labeled with TMRM.

more desensitization. The fluorescence remained steady as the current declined by more than 50%. Both α_1L127Cβ_2 receptors labeled with AF and α_1E122Cβ_2 receptors labeled with TMRM showed substantial decays in the current, while the fluorescence remained flat (Figure 6). Receptors with labels on the β_2 subunit produced smaller fluorescence changes; therefore, although the fluorescence appeared to remain flat as the receptor current decayed, the absence of fluorescence changes in β_2-subunit labels during desensitization was more difficult to judge (data not shown). The failure of the fluorescence to decline during desensitization suggests that the labeled residues in the ligand-binding pocket of the α_1 subunit do not change their environment significantly during transitions between the open and desensitized states. However, because fast desensitization cannot be seen with the relatively slow rate of drug application in recordings from oocytes, we cannot rule out the possibility that the initial fluorescence changes arise from a very rapidly generated desensitized conformation rather than open channels.

Competitive and Noncompetitive Antagonist Actions. SR-95531 is a competitive antagonist of the $GABA_A$ receptor, occupying the GABA-binding pocket without gating the channel. SR-95531 induced large fluorescence changes in labeled α_1L127C$\beta_2\gamma_2$ receptors, opposite in direction to those induced by GABA (Figure 7). Labeled α_1E122Cβ_2 and α_1E122C$\beta_2\gamma_2$ also showed fluorescence changes in response to SR95531 that were in the opposite direction to those produced by GABA. On the other hand, SR-95531 failed to induce fluorescence changes in labeled α_1L127Cβ_2 receptors

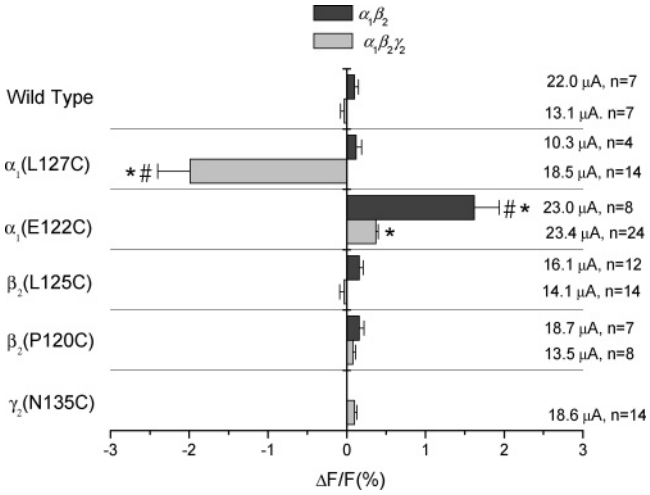

FIGURE 8: Average fluorescence changes in response to SR-95531. Each recording was performed with SR-95531 near IC_{99} to obtain maximum fluorescence changes. The peak fluorescence change was measured for each recording, and oocytes were tested with GABA as well. When the current induced by GABA was below 7 μA, no further experiments were performed on that oocyte. $\alpha_1\beta_2\gamma_2$L140C receptors were not included because currents were too low (~300 nA). The average peak GABA-activated current and number of oocytes are indicated to the right. The asterisk and pound sign indicate a significant difference from the wild type by the *t* test and one-way ANOVA, respectively.

even though GABA produced large signals (Figure 8). These results suggest that this competitive antagonist induces structural changes distinctly different from those that occur

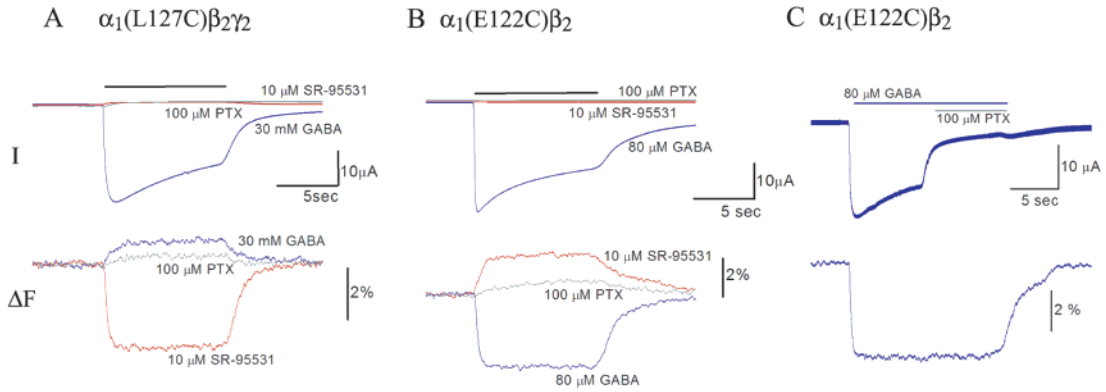

FIGURE 9: Simultaneous measurement of current and fluorescence in response to picrotoxin, SR-95531, and GABA. GABA was applied first to test for receptor expression, and then the two antagonists were applied successively to the same oocyte. Note that picrotoxin never produced a fluorescence change, but both antagonists produced small reductions in current when receptors contained the γ_2 subunit. (A) α_1L127C$\beta_2\gamma_2$ receptors labeled with TMRM. (B) α_1E122Cβ_2 receptors labeled with TMRM. (C) Picrotoxin does not block the fluorescence change induced by GABA in α_1E122Cβ_2 receptors labeled with TMRM.

during activation. However, we cannot exclude the possibility of the antagonist quenching the fluorophore through close proximity. This possibility could also explain why SR-95531 produced no fluorescence change in the β_2- and γ_2-subunit labels, which are not near the GABA-binding pocket. Although a direct interaction between the antagonist and label could account for some of the fluorescence changes, it would be difficult to explain the opposite changes in fluorescence of labels at residues 122 and 127.

The binding site of picrotoxin is believed to be formed by the M2 segment deep within the channel (*32*, *33*) and far from the GABA-binding pocket highlighted in Figure 1B. When we applied a high concentration of picrotoxin (100 μM $\approx EC_{95-99}$) to labeled mutant receptors, no fluorescence change was observed (Figure 9). This indicates that picrotoxin alone does not cause molecular rearrangements in the ligand-binding pocket of the $GABA_A$ receptor. Because GABA-bound desensitized receptors fluoresce with different intensities from GABA-free receptors (Figure 6), it would appear that picrotoxin does not induce a conformational transition similar to that seen during receptor desensitization. The possibility remains that picrotoxin induces an allosteric transition in other parts of the protein, and further labeling studies at different locations may reveal these sites.

Because picrotoxin blocks the gating transition in the ion-channel domain of the protein, we tested whether it can also block the conformational changes induced by GABA in the extracellular N terminus. In the presence of picrotoxin, GABA still induces a large fluorescence change (Figure 9C; N=6), indicating that the structural changes around the GABA-binding site can still occur even when the current is blocked. Thus, either these two domains of the $GABA_A$ receptor exhibit weak, easily disrupted coupling or, alternatively, picrotoxin can block the channel without inducing a structural transition, as might be expected for an open-channel block mechanism.

Both picrotoxin and SR-95531 produced a small diminution of current in the absence of GABA of approximately 0.5−1 μA when receptors contained the γ_2 subunit (Figure 9). This presumably reflects the block of current through spontaneously open $GABA_A$ receptor channels. The time course for this change indicates that picrotoxin binds in about 1 s. Because this current block occurs in the absence of GABA, picrotoxin probably binds rapidly to the inactive form of the receptor. However, it is conceivable that drug binding only to spontaneously open channels could reduce the current in the time observed. The fact that SR-95531 blocks spontaneous channel opening by binding to a site distant from the open channel suggests that spontaneous channel opening is a global transition dependent upon concomitant structural changes in the agonist-binding domains. Picrotoxin also blocked spontaneous channel opening but without producing changes at these labeled sites.

DISCUSSION

We have investigated ligand-induced structural transitions between the closed, open, and desensitized states in the $GABA_A$ receptor with site-specific fluorescence labels. This approach allowed us to monitor structural changes at selected locations during functional transitions in this LGIC. In this way, we were able to gain insight into the extent of the structural transition during GABA-induced channel opening and contrast this with the very different changes resulting from antagonist binding.

Origin of Fluorescence Changes. Changes in the fluorescence of molecules such as those used as labels here are widely interpreted in terms of a change in the polarity of the immediate environment of the label. This is the simplest interpretation and has been invoked in previous studies of fluorescent labels in LGICs (*9*, *10*). However, it is also possible that the conformational change alters the spatial relation between the fluorophore and a protein side chain with quenching activity. It is also possible that a ligand could alter fluorescence by a direct interaction. We cannot rigorously exclude these possibilities, but quenching interactions usually show chemical specificity and qualitatively similar results for two different fluorophores, rhodamine and alexa fluor 546, at two different sites, do not support such specificity. Furthermore, the different linker lengths for the two rhodamine labels (7.8 Å for MTSR and 5 Å for TMRM) should alter the specific environment of the fluorophore, but the fluorescence changes seen by these two labels were qualitatively similar (Figure 3). For the label at E122C of the α_1 subunit, a direct quenching by the ligand is less likely because this residue is further from the binding site (Figure 1) (*14*) and labels at this site still showed a large fluorescence change. Moreover, the labels on the β_2 subunit are clearly

too far away for a direct ligand interaction, and these labels showed the same qualitative pattern of fluorescence changes in response to GABA as labels on the homologous sites of the α_1 subunit.

The AF fluorophore differs from the rhodamine moiety of MTSR and TMRM in carrying a formal charge of −1. In a fluorometry study of the Shaker potassium channel, opposite fluorescence changes were seen in a mutant protein labeled with two different fluorophores (*34*) and it was suggested that the different charges might result in slightly different positions of the fluorophores and thus slightly different environments. Because in our study every comparison of AF with the other two labels showed qualitatively similar behavior, it is likely that the charge of the label has a smaller effect on the environment taken up by labels at the sites studied here in the $GABA_A$ receptor. The two α_1-subunit labels changed fluorescence in the opposite direction when GABA was applied, and fluorescence changes of both of these labels reversed sign when the competitive antagonist, SR-95531, was applied. These results are all consistent with the interpretation that these labels are reporting changes in the polarity of their environment.

Structural Changes and Receptor Activation. The interpretation of fluorescence in terms of environment polarity offers some interesting insights into the nature of structural changes during ligand binding. The side chain of residue 127 of the α_1-subunit faces into the GABA-binding cavity, and the fluorescence increase could indicate that ligand binding induces some degree of closure of this cavity through a shortening of the distance between loop E of the α subunit and the adjacent part of the β_2 subunit. SCAM studies of the $GABA_A$ receptor supported a similar ligand-binding pocket closure (*6*). A movement of this form is consistent with the idea that receptor activation entails a shortening of the distance between binding determinants residing on two adjacent subunits (*35*). A similar ligand-induced domain closure has also been observed in the GluR2 glutamate receptor (*36*), which belongs to a family of LGICs unrelated to the $GABA_A$ receptors and nAChRs. The side chain of residue 122 of the α_1 subunit is predicted to protrude from a loop linking β-strands 5 and 6, and residues in this region have been shown to influence receptor sensitivity (*37*). If this side chain faces away from the cavity, then cavity closure could increase the exposure of a label at this site and thus account for its fluorescence decrease. The pattern of fluorescence changes of labels at these two sites is thus consistent with the idea that GABA binding initiates a rigid-body movement of this section of the β sheet. The opposite pattern of movement, opening of the cavity, greater aqueous exposure of residue 127, and less exposure of residue 122 would then account for the pattern of fluorescence changes elicited by SR-95531. These results thus indicate that the position of this element of the putative β sheet with respect to the adjacent β subunit serves as an important determinant of the energetics of channel opening. This domain-closing motion may serve to initiate a conformational wave propagating to the channel domain, as envisioned in the nAChR (*38*).

On the basis of an electron microscope structure of the nAChR, agonist binding was proposed to initiate a domain rotation within the principle ligand-binding subunit (*39*). A mechanical link to the M2 segment of the same subunit was proposed to initiate channel gating. According to this hypothesis, the fluorescence changes in the β-subunit labels would likely follow channel opening. An alternative hypothesis can be put forward that an initial structural transition occurs cooperatively in the extracellular domains of all of the subunits, and this creates tension on all of the M2 segments to open the channel (*29*). Determining the temporal relationship between channel gating and the movements in the homologous regions of the extracellular domains of different subunits could then distinguish between these two distinct hypotheses for receptor activation.

Symmetry of Conformational Changes. The $GABA_A$ receptor is a hetero-oligomer, and in our study, we examined receptors composed from α_1 and β_2 subunits with and without the γ_2 subunit. The stoichiometry of $\alpha\beta\gamma$ $GABA_A$ receptors is 2:2:1 (*40*−*42*), but in $\alpha\beta$ $GABA_A$ receptors, the α_1 and β_2 subunits could be in ratios of either 3:2 (*43*, *44*) or 2:3 (*41*, *45*). Monod et al. (*22*) postulated a symmetrical transition in multisubunit proteins, but perfect symmetry cannot be realized in a hetero-oligomeric LGIC. The pseudosymmetrical character of these receptors raises questions about the extent of symmetry during the allosteric transitions of these proteins. Our study showed that residues of the α_1 subunit and homologous residues of the β_2 subunit of the $\alpha\beta$ $GABA_A$ receptor reported a similar pattern of fluorescence changes in response to GABA (Figures 2 and 5). Thus, in these domains, the transition shows some degree of symmetry. However, the magnitudes of the fluorescence changes in the labels of the β_2 subunit were smaller, and this difference is more difficult to interpret because of uncertainty regarding subunit stoichiometry (fewer β subunits), subunit nonequivalence within the pentameric structure, and labeling efficiency of different sites. Thus, we cannot distinguish between the two alternatives of smaller changes in the environment of the β_2-subunit labels during transitions and equal changes in environment, with other factors accounting for the difference in fluorescence changes. It is nevertheless significant that in these experiments some degree of symmetry is indicated between homologous sites on the two subunits.

Incorporating the γ_2 subunit changed the magnitudes of fluorescence changes in response to both agonist and antagonist at most of the sites labeled (Figures 5 and 8), with both α_1 and β_2 subunits reporting nearly 3-fold lower fluorescence changes in response to GABA. The pattern of fluorescence changes seen in labels at homologous sites on the α_1 and β_2 subunits in the $\alpha\beta$ $GABA_A$ receptor was essentially lost in $\alpha\beta\gamma$ $GABA_A$ receptors. The reduced fluorescence changes in α_1-subunit labels indicate that the γ_2 subunit induces structural changes that propagate through adjacent subunits of the $GABA_A$ receptor. The higher EC_{50} values in $GABA_A$ receptors containing the γ_2 subunit (Table 1) (*46*, *47*) thus may result from a change in binding as well as a change in the gating equilibrium. The observation that fluorescence signals in both the α_1 and β_2 subunits were reduced suggests that the γ_2 subunit can allow gating to occur with smaller structural changes in the extracellular domains.

A label at a homologous site in the γ_2 subunit showed no significant fluorescence change, even though this receptor expressed very well (N135Cγ_2 in Figure 5). This further indicates that the $\alpha\beta\gamma$ receptor fails to conserve the partially symmetric character of the transition seen in $\alpha\beta$ receptors.

The fact that the α_1 subunit is more homologous to the γ_2 subunit than to the β_2 subunit (*48*) makes this a particularly intriguing result because it implies that sequence homology does not translate into homology of structure nor does it translate into homology of the structural changes induced by ligand binding.

Molecular Rearrangements during Desensitization. During transitions from the open to desensitized states, the labels on the α_1 subunit (Figure 6) and homologous residues of the β_2 subunit show relatively little change in their environment. Because both the open and desensitized states are induced by ligand binding, they should have a high affinity. From that perspective, the absence of structural changes in or near the GABA-binding pocket is reasonable. Presumably, structural changes occur during this transition but in different parts of the protein. Changes must occur in the pore-lining M2 segment because the channel is closed in the desensitized state. However, a similar experiment in the nAChR showed that a label at the extracellular end of the M2 segment of the β subunit increased its fluorescence during channel opening and also failed to change its fluorescence further during desensitization (*10*). Knowing which residues undergo structural changes during this transition will clarify the mechanism of LGIC desensitization, and it is hoped that further experiments with fluorescent probes will identify these parts of the protein.

Antagonist-Induced Fluorescence Changes. We tested two antagonists with different modes of action, SR-95531 and picrotoxin. The competitive antagonist SR-95531 induced large fluorescence changes in α_1-subunit labels that were opposite in sign to those produced by GABA, and these fluorescence changes at least partly reflect changes in the structure of the ligand-binding pocket. A SCAM study showed that SR-95531 increases the accessibility of a residue lining the ligand-binding pocket in the β subunit (*7*), further supporting the interpretation that this drug induces a significant structural change in the ligand-binding pocket. These results argue that this antagonist does more than simply occlude the binding site and prevent GABA binding. This then implies some conformational flexibility in the binding pocket, with motions not restricted solely to those associated with channel opening. Competitive antagonists have also been reported to induce changes in the fluorescence of labels in the AChBP (*19*) and the $GABA_C$ receptor (*9*).

Picrotoxin binds to a site of the receptor that is not involved in agonist binding. A site deep in the M2 segment has been indicated for a *Drosophila* $GABA_A$ receptor homologue, and in this study, a dual mechanism was proposed with picrotoxin blocking the ion-conduction pathway as well as preferentially binding to the desensitized state (*49*). A SCAM study performed on the $GABA_A$ receptor showed that application of picrotoxin blocked the GABA-dependent reaction of an MTSR reagent with a residue very near the cytoplasmic end of the M2 segment (α_1V257C) (*33*). In the present study, picrotoxin failed to induce fluorescence changes in labels that were strongly influenced by drugs that bound to the GABA-binding site. Similar results were reported in a fluorescent label study of the $GABA_C$ receptor (*9*), but this receptor shows relatively weak desensitization. The negative result in the present study with a receptor showing stronger desensitization thus strengthens the conclusion that the structural changes associated with picrotoxin are more limited. Limited structural changes induced by picrotoxin are further supported by the failure of picrotoxin to reverse the fluorescence changes in the label induced by GABA (Figure 9C). If picrotoxin does induce a global transition, this transition differs from that seen during desensitization, especially in the ligand-binding pocket of the extracellular domain. The structural transition induced by picrotoxin may be confined to the channel-forming domains of the protein.

SR-95531 and picrotoxin both blocked spontaneous openings of the GABA receptor (Figure 9). In the case of SR-95531, the structural changes in the ligand-binding pocket inferred from the fluorescence changes in α_1-subunit labels (Figures 7 and 8) may raise the energy barrier to spontaneous channel opening. Thus, spontaneous opening is still a global transition, accompanied by changes extending to the ligand-binding pocket. However, picrotoxin can block spontaneous opening without producing such extensive structural changes.

CONCLUSIONS

Fluorescent labels in and near the ligand-binding pocket of the α_1 subunit and homologous sites on the β_2 and γ_2 subunits far from the ligand-binding pocket have provided insight into how different parts of the $GABA_A$ receptor protein change during functional transitions. The structural changes associated with transitions induced by GABA are more extensive for $\alpha\beta$ receptors than for $\alpha\beta\gamma$ receptors and more extensive than for transitions induced by antagonists. The capacity of ligands to influence the function of LGICs can thus result from structural changes that vary in extent. Allosteric transitions are generally viewed as more extensive global changes in the protein structure. The relative contribution of global and local changes may be an important characteristic of the modulation of function of LGICs. Further studies with fluorescent labels will advance our understanding of this important aspect of LGIC function.

ACKNOWLEDGMENT

We thank Andrew Boileau and other members of the Jackson and Czajkowski research groups for valuable discussions and advice throughout the course of this study. We thank Ken Satyshur for computer modeling and Jeff Walker and Gerard Marriott for helpful discussions.

REFERENCES

1. Akabas, M. H., Stauffer, D. A., Xu, M., and Karlin, A. (1992) Acetylcholine receptor channel structure probed in cysteine-substitution mutants, *Science 258*, 307−310.
2. Akabas, M. H., Kaufmann, C., Archdeacon, P., and Karlin, A. (1994) Identification of acetylcholine receptor channel-lining residues in the entire M2 segment of the α subunit, *Neuron 13*, 919−927.
3. Xu, M., and Akabas, M. H. (1996) Identification of channel-lining residues in the M2 membrane-spanning segment of the $GABA_A$ receptor α_1 subunit, *J. Gen. Physiol. 107*, 195−205.
4. Karlin, A., and Akabas, M. H. (1998) Substituted-cysteine accessibility method, *Methods Enzymol. 293*, 123−145.
5. Boileau, A. J., Evers, A. R., Davis, A. F., and Czajkowski, C. (1999) Mapping the agonist binding site of the $GABA_A$ receptor: Evidence for a β-strand, *J. Neurosci. 19*, 4847−4854.
6. Wagner, D. A., and Czajkowski, C. (2001) Structure and dynamics of the GABA binding pocket: A narrowing cleft that constricts during activation, *J. Neurosci. 21*, 67−74.
7. Boileau, A. J., Newell, J. G., and Czajkowski, C. (2002) $GABA_A$ receptor β_2 Tyr97 and Leu99 line the GABA-binding site. Insights

into mechanisms of agonist and antagonist actions, *J. Biol. Chem. 277*, 2931−2937.
8. Holden, J. H., and Czajkowski, C. (2002) Different residues in the $GABA_A$ receptor α_1T60−α_1K70 region mediate GABA and SR-95531 actions, *J. Biol. Chem. 277*, 18785−18792.
9. Chang, Y., and Weiss, D. S. (2002) Site-specific fluorescence reveals distinct structural changes with GABA receptor activation and antagonism, *Nat. Neurosci. 5*, 1163−1168.
10. Dahan, D. S., Dibas, M. I., Petersson, E. J., Auyeung, V. C., Chanda, B., Bezanilla, F., Dougherty, D. A., and Lester, H. A. (2004) A fluorophore attached to nicotinic acetylcholine receptor β M2 detects productive binding of agonist to the $\alpha\delta$ site, *Proc. Natl. Acad. Sci. U.S.A. 101*, 10195−10200.
11. Barnard, E. A., Skolnick, P., Olsen, R. W., Mohler, H., Sieghart, W., Biggio, G., Braestrup, C., Bateson, A. N., and Langer, S. Z. (1998) International Union of Pharmacology. XV. Subtypes of γ-aminobutyric $acid_A$ receptors: Classification on the basis of subunit structure and receptor function, *Pharmacol. Rev. 50*, 291−313.
12. Sixma, T. K., and Smit, A. B. (2003) Acetylcholine binding protein (AChBP): A secreted glial protein that provides a high-resolution model for the extracellular domain of pentameric ligand-gated ion channels, *Annu. Rev. Biophys. Biomol. Struct. 32*, 311−334.
13. Cromer, B. A., Morton, C. J., and Parker, M. W. (2002) Anxiety over $GABA_A$ receptor structure relieved by AChBP, *Trends Biochem. Sci. 27*, 280−287.
14. Ernst, M., Bruckner, S., Boresch, S., and Sieghart, W. (2005) Comparative models of $GABA_A$ receptor extracellular and transmembrane domains: Important insights in pharmacology and function, *Mol. Pharmacol. 68*, 1291−1300.
15. Horenstein, J., Wagner, D. A., Czajkowski, C., and Akabas, M. H. (2001) Protein mobility and GABA-induced conformational changes in $GABA_A$ receptor pore-lining M2 segment, *Nat. Neurosci. 4*, 477−485.
16. Lester, H. A., Dibas, M. I., Dahan, D. S., Leite, J. F., and Dougherty, D. A. (2004) Cys-loop receptors: New twists and turns, *Trends Neurosci. 27*, 329−336.
17. Karlin, A. (2002) Emerging structure of the nicotinic acetylcholine receptors, *Nat. Rev. Neurosci. 3*, 102−114.
18. Brejc, K., van Dijk, W. J., Klaassen, R. V., Schuurmans, M., van der Oost, J., Smit, A. B., and Sixma, T. K. (2001) Crystal structure of an ACh-binding protein reveals the ligand-binding domain of nicotinic receptors, *Nature 411*, 269−276.
19. Hibbs, R. E., Talley, T. T., and Taylor, P. (2004) Acrylodan-conjugated cysteine side chains reveal conformational state and ligand site locations of the acetylcholine-binding protein, *J. Biol. Chem. 279*, 28483−28491.
20. Gao, F., Bren, N., Burghardt, T. P., Hansen, S., Henchman, R. H., Taylor, P., McCammon, J. A., and Sine, S. M. (2005) Agonist-mediated conformational changes in acetylcholine-binding protein revealed by simulation and intrinsic tryptophan fluorescence, *J. Biol. Chem. 280*, 8443−8451.
21. Akabas, M. H. (2004) $GABA_A$ receptor structure−function studies: A reexamination in light of new acetylcholine receptor structures, *Int. Rev. Neurobiol. 62*, 1−43.
22. Monod, J., Wyman, J., and Changeux, J. (1965) On the nature of allosteric transitions: A plausible model, *J. Mol. Biol. 12*, 88−118.
23. Koshland, D. E., Nemethy, G., and Filmer, D. (1966) Comparison of experimental binding data and theoretical models in proteins containing subunits, *Biochemistry 5*, 365−384.
24. Henchman, R. H., Wang, H. L., Sine, S. M., Taylor, P., and McCammon, J. A. (2005) Ligand-induced conformational change in the α7 nicotinic receptor ligand binding domain, *Biophys. J. 88*, 2564−2576.
25. Liman, E. R., Tytgat, J., and Hess, P. (1992) Subunit stoichiometry of a mammalian K^+ channel determined by construction of multimeric cDNAs, *Neuron 9*, 861−871.
26. Boileau, A. J., Kucken, A. M., Evers, A. R., and Czajkowski, C. (1998) Molecular dissection of benzodiazepine binding and allosteric coupling using chimeric γ-aminobutyric $acid_A$ receptor subunits, *Mol. Pharmacol. 53*, 295−303.
27. Mannuzzu, L. M., Moronne, M. M., and Isacoff, E. Y. (1996) Direct physical measure of conformational rearrangement underlying potassium channel gating, *Science 271*, 213−216.
28. Laskowski, R. A., MacArthur, M. W., Moss, D. S., and Thornton, J. M. (1993) PROCHECK: A program to check the stereochemical quality of protein structures, *J. Appl. Crystallogr. 26*, 283−291.
29. Corringer, P. J., Le Novere, N., and Changeux, J. P. (2000) Nicotinic receptors at the amino acid level, *Annu. Rev. Pharmacol. Toxicol. 40*, 431−458.
30. Holden, J. H., and Czajkowski, C. (2001) Mapping agonist and antagonist binding site subdomains in the α_1M113−T125 region of the $GABA_A$ receptor, *Soc. Neurosci. Abstracts 31*, 35.7.
31. Holden, J. H., and Czajkowski, C. (2003) α_1Gly^{124}−α_1Leu^{132}: A novel binding site region on the $GABA_A$ receptor that undergoes distinct conformational rearrangements during ligand binding and allosteric modulation, *Soc. Neurosci. Abstracts 33*, 50.10.
32. Zhang, H.-G., ffrench-Constant, R. H., and Jackson, M. B. (1994) A unique amino acid of the *Drosophila* GABA receptor determines drug sensitivity by two mechanisms, *J. Physiol. 479*, 65−75.
33. Xu, M., Covey, D. F., and Akabas, M. H. (1995) Interaction of picrotoxin with $GABA_A$ receptor channel-lining residues probed in cysteine mutants, *Biophys. J. 69*, 1858−1867.
34. Cha, A., and Bezanilla, F. (1997) Characterizing voltage-dependent conformational changes in the Shaker K^+ channel with fluorescence, *Neuron 19*, 1127−1140.
35. Karlin, A., and Akabas, M. H. (1995) Toward a structural basis for the function of nicotinic acetylcholine receptors and their cousins, *Neuron 15*, 1231−1244.
36. Armstrong, N., and Gouaux, E. (2000) Mechanisms for activation and antagonism of an AMPA-sensitive glutamate receptor: Crystal structures of the GluR2 ligand binding core, *Neuron 28*, 165−181.
37. Westh-Hansen, S. E., Rasmussen, P. B., Hastrup, S., Nabekura, J., Noguchi, K., Akaike, N., Witt, M. R., and Nielsen, M. (1997) Decreased agonist sensitivity of human $GABA_A$ receptors by an amino acid variant, isoleucine to valine, in the α_1 subunit, *Eur. J. Pharmacol. 329*, 253−257.
38. Grosman, C., Zhou, M., and Auerbach, A. (2000) Mapping the conformational wave of acetylcholine receptor channel gating, *Nature 403*, 773−776.
39. Miyazawa, A., Fujiyoshi, Y., and Unwin, N. (2003) Structure and gating mechanism of the acetylcholine receptor pore, *Nature 423*, 949−955.
40. Chang, Y., Wang, R., Barot, S., and Weiss, D. S. (1996) Stoichiometry of a recombinant $GABA_A$ receptor, *J. Neurosci. 16*, 5415−5424.
41. Tretter, V., Ehya, N., Fuchs, K., and Sieghart, W. (1997) Stoichiometry and assembly of a recombinant $GABA_A$ receptor subtype, *J. Neurosci. 17*, 2728−2737.
42. Farrar, S. J., Whiting, P. J., Bonnert, T. P., and McKernan, R. M. (1999) Stoichiometry of a ligand-gated ion channel determined by fluorescence energy transfer, *J. Biol. Chem. 274*, 10100−10104.
43. Im, W. B., Pregenzer, J. F., Binder, J. A., Dillon, G. H., and Alberts, G. L. (1995) Chloride channel expression with the tandem construct of $\alpha_6\beta_2$ $GABA_A$ receptor subunit requires a monomeric subunit of α_6 or γ_2, *J. Biol. Chem. 270*, 26063−26066.
44. Boileau, A. J., Pearce, R. A., and Czajkowski, C. (2005) Tandem subunits effectively constrain $GABA_A$ receptor stoichiometry and recapitulate receptor kinetics but are insensitive to $GABA_A$ receptor-associated protein, *J. Neurosci. 25*, 11219−11230.
45. Horenstein, J., and Akabas, M. H. (1998) Location of a high affinity Zn^{2+} binding site in the channel of $\alpha_1\beta_1\gamma$-aminobutyric $acid_A$ receptors, *Mol. Pharmacol. 53*, 870−877.
46. Boileau, A. J., Li, T., Benkwitz, C., Czajkowski, C., and Pearce, R. A. (2003) Effects of γ_{2S} subunit incorporation on $GABA_A$ receptor macroscopic kinetics, *Neuropharmacology 44*, 1003−1012.
47. Boileau, A. J., Baur, R., Sharkey, L. M., Sigel, E., and Czajkowski, C. (2002) The relative amount of cRNA coding for γ_2 subunits affects stimulation by benzodiazepines in $GABA_A$ receptors expressed in *Xenopus* oocytes, *Neuropharmacology 43*, 695−700.
48. Whiting, P. J., Bonnert, T. P., McKernan, R. M., Farrar, S., Le Bourdelles, B., Heavens, R. P., Smith, D. W., Hewson, L., Rigby, M. R., Sirinathsinghji, D. J., Thompson, S. A., and Wafford, K. A. (1999) Molecular and functional diversity of the expanding GABA-A receptor gene family, *Ann. N.Y. Acad. Sci. 868*, 645−653.
49. Zhang, H.-G., ffrench-Constant, R. H., and Jackson, M. B. (1994) A unique amino acid of the *Drosophila* GABA receptor influences drug sensitivity by two mechanisms, *J. Physiol. 479*, 65−75.

BI060222V